

Fermion–charged-boson stars

Ben Kain

Department of Physics, College of the Holy Cross, Worcester, Massachusetts 01610, USA

Fermion-boson stars are starlike systems composed of the ordinary nuclear matter of a neutron star and bosonic dark matter. The bosonic dark matter has typically been taken to be a complex scalar field. A natural extension is for the complex scalar field to be charged. We make the simplest extension and gauge the scalar field under $U(1)$. We therefore study fermion–charged-boson stars. We make a detailed study of the stability of this system by computing critical curves over the whole of parameter space. We then study how the fermion and boson sectors contribute to the total mass of the star. Finally, we present mass-radius diagrams, showing that an increase in charge can lead to more massive and more compact stars.

I. INTRODUCTION

Fermion-boson stars are starlike configurations made up of a mixture of fermions and bosons [1]. The fermion sector is described by a perfect fluid energy-momentum tensor and an equation of state [2]. Typically, one uses an equation of state that can describe the nuclear matter in a neutron star. The boson sector is most commonly taken to be a complex scalar field. By itself, a complex scalar field can form boson stars [3–7].

Dark matter direct detection experiments have placed stringent constraints on the dark matter-nucleon coupling strength [8–10]. From the perspective of fermion-boson stars, it is generally assumed that the coupling strength is negligibly small and that there exists only gravitational interactions between the fermion and boson sectors.

Fermion-boson stars are therefore examples of dark matter admixed neutron stars [1, 11, 12] with bosonic dark matter. It is a theoretical possibility that during the formation process of a neutron star, dark matter could become mixed with ordinary matter in sufficient quantities to affect bulk properties of the star, such as its mass and radius. Neutron stars, then, offer the exciting possibility of indirectly probing dark matter.

Fermion-boson stars were first studied by Henriques, Liddle, and Moorhouse [1, 13, 14]. In these works, the fermion sector was a free Fermi gas of neutrons and the boson sector was a neutral complex scalar field. More recently, these systems have been evolved with full numerical relativity, with the fermion sector described by a polytropic equation of state and the boson sector again taken to be a neutral complex scalar field [15–18]. For additional work on fermion-boson stars, see [19–26].

Since the scalar field is complex, a natural extension is for the scalar field to be charged. We make the simplest extension and gauge the scalar field under $U(1)$ so that the scalar field interacts with dark photons. By themselves, such charged scalar fields can form charged boson stars [27, 28]. When mixed with fermions, then, they can form fermion–charged-boson stars.

A useful dimensionless quantity for understanding the relative mass scales for the fermion and boson sectors can

be shown to be [1]

$$\beta \equiv \frac{(\mu_N/m_P)^2}{\mu/m_P}, \quad (1)$$

where m_P is the Planck mass, μ is the scalar field particle mass, and μ_N is the representative particle mass for the fermion sector, which we take to be the nucleon mass $\mu_N = 938$ MeV. Roughly speaking, when β is order one, there is a single mass scale in the system and the fermion and boson sectors can both be non-negligible [1]. For order one β , we have $\mu \sim 10^{-10}$ eV. Thus, fermion-boson stars are most interesting with ultralight bosonic dark matter [1, 29–31]. This is not unexpected, since it is well-known that boson stars take on astrophysical sizes, with masses in the solar mass range and radii in the kilometer range, when the scalar field mass is ultralight [7].

In this paper, we study static solutions of spherically symmetric fermion–charged-boson stars. We use a realistic equation of state in the fermion sector. In the boson sector, we focus on a scalar field with mass 10^{-10} eV, but at times will also consider larger masses. In Sec. II, we present two parametrizations for the spherically symmetric metric that we will be using and the equations for determining the metric functions. As mentioned above, we assume that there exists only gravitational interactions between the fermion and boson sectors. Consequently, the equations of motion for the two sectors can be derived independently. In Sec. III, we review fermion stars, for which the equations of motion are the Tolman-Oppenheimer-Volkoff (TOV) equations. In doing this, we use the NL3 equation of state [32, 33], which is a realistic equation of state for the nuclear matter in a neutron star. We detail how this equation of state is constructed in the Appendix. In Sec. IV, we review charged boson stars. We take special care to explain how a particular gauge choice leads to all fields being time-independent. In Sec. V, we combine the equations presented in Secs. III and IV and study fermion–charged-boson stars. In addition to solving the equations for static solutions and presenting mass-radius diagrams, there are two important questions we address. The first concerns the stability of the static solutions. We use the two-fluid methods developed in [14] and determine stability over the whole of parameter space. The second question concerns the relative contri-

butions from the fermion and boson sectors. We study this issue by looking at the relative contributions to the total mass of the star. In this way, we show that as the mass of the scalar field particle is increased, the transition from being fermion dominated to being boson dominated sharpens. We conclude in Sec. VI.

II. METRIC AND METRIC EQUATIONS

We focus on spherically symmetric spacetimes and use units such that $c = \hbar = 1$. We will make use of two parametrizations of the spherically symmetric metric. One parametrization is

$$ds^2 = -\alpha^2 dt^2 + a^2 dr^2 + r^2(d\theta^2 + \sin^2\theta d\phi^2), \quad (2)$$

where α and a are metric functions determined from the Einstein field equations,

$$G^\mu{}_\nu = 8\pi G(T_{\text{tot}})^\mu{}_\nu, \quad (3)$$

where $G^\mu{}_\nu$ is the Einstein tensor, G is the gravitational constant, and $(T_{\text{tot}})^\mu{}_\nu$ is the energy-momentum tensor.

In Sec. V, we consider fermion-charged-boson stars and $(T_{\text{tot}})^\mu{}_\nu$ will have both fermionic and bosonic contributions,

$$(T_{\text{tot}})^\mu{}_\nu = (T_f)^\mu{}_\nu + (T_b)^\mu{}_\nu. \quad (4)$$

That the two contributions separate follows from our assumption that there exists only gravitational interactions between the fermion and boson sectors. In Sec. III, we review fermion stars, in which the energy-momentum tensor has only the fermionic contribution, and in Sec. IV, we review charged bosons stars, in which the energy-momentum tensor has only the bosonic contribution. Since the two contributions in Eq. (4) are independently conserved, $\nabla_\mu(T_f)^\mu{}_\nu = 0$ and $\nabla_\mu(T_b)^\mu{}_\nu = 0$, where ∇_μ is the metric-covariant derivative, the equations derived in the next two sections will be directly applicable to fermion-charged-boson stars.

The Einstein field equations lead to the following equations for determining α and a ,

$$\begin{aligned} \frac{\alpha'}{\alpha} &= +4\pi G r a^2 (T_{\text{tot}})^r{}_r + \frac{a^2 - 1}{2r} \\ \frac{a'}{a} &= -4\pi G r a^2 (T_{\text{tot}})^t{}_t - \frac{a^2 - 1}{2r} \\ \frac{\dot{a}}{a} &= -4\pi G r \alpha^2 (T_{\text{tot}})^t{}_r, \end{aligned} \quad (5)$$

where a prime denotes an r derivative and a dot denotes a t derivative.

When solving for static solutions, an alternative parametrization of the metric is useful, which is

$$ds^2 = -\sigma^2 N dt^2 + \frac{dr^2}{N} + r^2(d\theta^2 + \sin^2\theta d\phi^2), \quad (6)$$

where $N \equiv 1 - 2Gm/r$ and the new metric functions are

$$\sigma \equiv \alpha a, \quad m \equiv \frac{r}{2G} \left(1 - \frac{1}{a^2}\right). \quad (7)$$

Using the first two equations in (5), σ and m obey

$$\begin{aligned} \frac{\sigma'}{\sigma} &= \frac{4\pi G r}{N} [(T_{\text{tot}})^r{}_r - (T_{\text{tot}})^t{}_t] \\ m' &= -4\pi r^2 (T_{\text{tot}})^t{}_r. \end{aligned} \quad (8)$$

We will also need

$$\frac{\alpha'}{\alpha} = \frac{4\pi G r^3 (T_{\text{tot}})^r{}_r + Gm}{r^2 N}, \quad (9)$$

which follows directly from the first equation in (5).

III. FERMION STARS

In this section, we review fermion stars. The equations derived here will be directly applicable to fermion-charged-boson stars. Our interest is with static solutions, for which spacetime is time-independent. For fermion stars, this immediately leads to all quantities being time-independent (things are not as straightforward for charged bosons stars, as we will see in the next section).

Fermion stars are described by a perfect fluid energy-momentum tensor [2],

$$(T_f)^\mu{}_\nu = \text{diag}(-\epsilon, p, p, p), \quad (10)$$

where ϵ is the energy density and p is the pressure of the fluid. Conservation of the energy-momentum tensor, $\nabla_\mu(T_f)^\mu{}_\nu = 0$, leads to the equation of motion,

$$p' = -\frac{\alpha'}{\alpha}(\epsilon + p). \quad (11)$$

Equation (11) and Eqs. (8) and (9) with $(T_{\text{tot}})^\mu{}_\nu = (T_f)^\mu{}_\nu$ are the TOV equations. Note that σ decouples and does not have to be computed if it is not needed.

In addition to the energy-momentum tensor, fermion stars are described by an equation of state, $\epsilon = \epsilon(p)$. We use the NL3 equation of state [32, 33], which is a realistic equation of state for neutron stars. We do not have a particular reason for choosing NL3, aside from it being realistic, and we expect the qualitative aspects of our results to hold for other choices. Nevertheless, for completeness, we review the construction of NL3 in the Appendix.

To solve the TOV equations, we need inner boundary conditions. Inner boundary conditions can be obtained by plugging Taylor expansions of the fields into the TOV equations, which gives $p(r) = p(0) + O(r^2)$ and $m(r) = O(r^3)$. Fermion stars are uniquely identified by the central pressure, $p(0)$. We thus specify a central pressure and then integrate Eq. (11) and the bottom equation

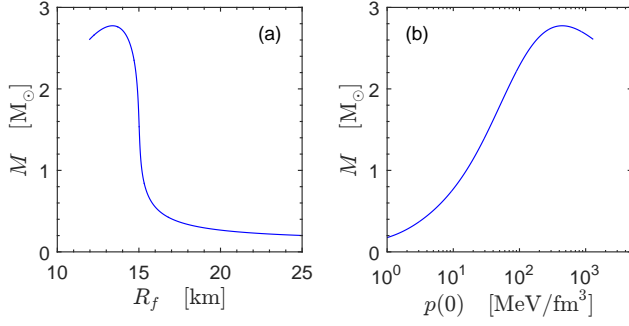


FIG. 1. (a) The mass-radius curve and (b) the mass as a function of the central pressure for fermion stars with the NL3 equation of state.

in (8) outward from $r = 0$. At each integration step we know the pressure and we compute the energy density using the equation of state. The radius of the star, R_f , is defined by the radial position at which the pressure hits zero, $p(R_f) = 0$, and the mass of the star is given by $M = m(R_f)$.

Some results are shown in Fig. 1. In Fig. 1(a) we show the mass-radius curve and in Fig. 1(b) we show the mass as a function of the central pressure. It is well-known that for a single-fluid system, such as considered in this section, the transition from stable to unstable occurs at the solution with the largest mass [2], which is called the critical solution. A solution with a central pressure smaller than the critical pressure is stable, otherwise it is unstable. The critical solution (for the NL3 equation of state that we are using) has $p(0) = 441$ MeV/fm³, $M = 2.78 M_\odot$, and $R_f = 13.4$ km.

IV. CHARGED BOSON STARS

In this section, we review charged boson stars [27]. The equations derived here will be directly applicable to fermion-charged-boson stars. We begin with the standard Lagrangian for a complex scalar field gauged under $U(1)$,

$$\mathcal{L}_b = -(D_\mu \phi)(D^\mu \phi)^* - V(|\phi|) - \frac{1}{4} F_{\mu\nu} F^{\mu\nu}, \quad (12)$$

where ϕ is the complex scalar field,

$$\begin{aligned} D_\mu \phi &= \partial_\mu \phi - ig A_\mu \phi \\ F_{\mu\nu} &= \partial_\mu A_\nu - \partial_\nu A_\mu \\ V &= \mu^2 |\phi|^2 + \lambda |\phi|^4, \end{aligned} \quad (13)$$

A_μ is the gauge field and is real, with $F_{\mu\nu}$ its field strength, μ is the scalar field particle mass, λ is the self-coupling constant, and g is the boson charge. For completeness, we derive equations for arbitrary λ , but, for simplicity, present results only for $\lambda = 0$. In spherically symmetric systems,

$$A_\mu = (A_t, A_r, 0, 0), \quad (14)$$

and the only nonzero components of the field strength are $F_{tr} = -F_{rt} = \partial_t A_r - \partial_r A_t$. For convenience, we give the flat space equations of motion for the scalar and gauge fields,

$$\begin{aligned} 0 &= D_\mu D^\mu \phi - \frac{dV}{d|\phi|^2} \phi \\ 0 &= \partial_\mu F^{\mu\nu} - J^\nu, \end{aligned} \quad (15)$$

which are the (gauged) Klein-Gordon and Maxwell equations, and where

$$J^\mu = ig \left[\phi^* D^\mu \phi - \phi (D^\mu \phi)^* \right] \quad (16)$$

is the conserved matter current. That it is conserved follows immediately from $F^{\mu\nu}$ being antisymmetric. The Lagrangian in Eq. (12) is invariant under a $U(1)$ transformation,

$$\phi \rightarrow \phi' = e^{-i\Lambda} \phi, \quad A_\mu \rightarrow A'_\mu = A_\mu - \frac{1}{g} \partial_\mu \Lambda, \quad (17)$$

where Λ is the gauge parameter. This allows for some freedom in how we parametrize ϕ and A_μ . We shall make a particular gauge choice below that is convenient for finding static solutions.

We minimally couple the Lagrangian in Eq. (12) to gravity via $\mathcal{L}_b \rightarrow \sqrt{-\det(g_{\mu\nu})} \mathcal{L}_b$, where $\det(g_{\mu\nu})$ is the determinant of the metric. The energy-momentum tensor is given by

$$\begin{aligned} (T_f)^\mu{}_\nu &= (D^\mu \phi)(D_\nu \phi)^* + (D^\nu \phi)^*(D_\mu \phi) \\ &\quad - \delta_\nu^\mu (D_\sigma \phi)(D^\sigma \phi)^* - \delta_\nu^\mu V \\ &\quad + F^{\mu\sigma} F_{\nu\sigma} - \frac{1}{4} \delta_\nu^\mu F_{\sigma\lambda} F^{\sigma\lambda}. \end{aligned} \quad (18)$$

The equations of motion may be obtained directly from the Lagrangian $\sqrt{-\det(g_{\mu\nu})} \mathcal{L}_b$ or by elevating the derivatives in Eq. (15) to derivatives covariant with respect to gravity. In writing the equations of motion and the components of the energy-momentum tensor, it is convenient to define

$$\mathcal{Q} \equiv -\frac{4\pi r^2}{\alpha a} F_{tr} = -\frac{4\pi r^2}{\alpha a} (\partial_t A_r - \partial_r A_t). \quad (19)$$

We shall find below that \mathcal{Q} gives the total charge inside a radius r . We note that we have defined $F_{tr} \equiv \partial_t A_r - \partial_r A_t$, with lower indices, from which $F^{tr} = -F_{tr}/(\alpha^2 a^2)$. The equations of motion are then

$$\begin{aligned} \partial_t \left(\frac{a}{\alpha} D_t \phi \right) &= \frac{1}{r^2} \partial_r \left(\frac{r^2 \alpha}{a} D_r \phi \right) + ig \left(\frac{a}{\alpha} A_t D_t \phi - \frac{\alpha}{a} A_r D_r \phi \right) \\ &\quad - \alpha a \frac{dV}{d|\phi|^2} \phi \\ \dot{\mathcal{Q}} &= +4\pi \alpha a r^2 J^r \\ \mathcal{Q}' &= -4\pi \alpha a r^2 J^t, \end{aligned} \quad (20)$$

where $D_\mu\phi$ is as given in Eq. (13) and

$$\begin{aligned} J^t &= -\frac{ig}{\alpha^2} [\phi^* D_t\phi - \phi(D_t\phi)^*] \\ J^r &= +\frac{ig}{\alpha^2} [\phi^* D_r\phi - \phi(D_r\phi)^*]. \end{aligned} \quad (21)$$

The energy-momentum tensor components that we will be using are

$$\begin{aligned} (T_b)^t_t &= -\frac{1}{\alpha^2} |D_t\phi|^2 - \frac{1}{a^2} |D_r\phi|^2 - V - \frac{\mathcal{Q}^2}{32\pi^2 r^4} \\ (T_b)^r_r &= +\frac{1}{\alpha^2} |D_t\phi|^2 + \frac{1}{a^2} |D_r\phi|^2 - V - \frac{\mathcal{Q}^2}{32\pi^2 r^4} \\ (T_b)^t_r &= -\frac{1}{\alpha^2} [(D_t\phi)(D_r\phi)^* + (D_t\phi)^* D_r\phi]. \end{aligned} \quad (22)$$

As mentioned, static solutions require the metric and energy-momentum tensor to be time independent. A look at the \dot{a} equation in (5) shows that we must also have $(T_b)^t_r = 0$. The best gauge to use when finding static solutions is radial gauge, for which

$$A_r = 0. \quad (23)$$

For the energy-momentum tensor to be time-independent, it follows from Eqs. (22) that $|D_t\phi|^2$ and \mathcal{Q} are time-independent, which leads to A_t being time-independent and $\phi = \phi(r)e^{-i\omega t}$ for complex $\phi(r)$ and real constant ω . A simple gauge transformation, with gauge parameter $\Lambda = \omega t$, removes the time-dependence of ϕ , while retaining $A_r = 0$ and shifting A_t by a constant, which we absorb into A_t .

A more complicated gauge transformation transforms ϕ to be purely real, as we now explain. We have just established that $\phi = \phi(r)$. This can be written in terms of real and imaginary parts or in terms of a modulus and phase,

$$\phi(r) = \phi_r(r) + i\phi_i(r) = |\phi(r)|e^{i \tan^{-1}[\phi_i(r)/\phi_r(r)]}. \quad (24)$$

Making a gauge transformation with gauge parameter $\Lambda = -\tan^{-1}(\phi_i/\phi_r)$ transforms ϕ to be purely real. Since ϕ_r, ϕ_i are time-independent, $\partial_t\Lambda = 0$ and A_t is unchanged. It is also the case that $\partial_r\Lambda = 0$ and we stay in radial gauge with $A_r = 0$. To show this, we have from $\dot{\mathcal{Q}} = 0$ in Eq. (20) that $J^r = 0$ and thus that $\phi^* D_r\phi = \phi(D_r\phi)^*$ which, with $A_r = 0$, becomes $\phi_r\phi'_i = \phi'_r\phi_i$. This is the necessary result to show that both $\partial_r\Lambda = 0$ and $(T_b)^t_r = 0$.

By making convenient gauge choices, we have that all fields (both metric and matter fields) are time-independent, that ϕ is real, and that $A_r = 0$. When presenting results, it is best to present gauge-independent quantities, which are $|\phi|$ and F_{tr} . From (19), \mathcal{Q} is also gauge-independent. The equations for the neutral boson star are obtained in the limit $g \rightarrow 0$. Since our gauge choice has absorbed a constant into A_t that is proportional to $1/g$, this limit is more easily taken after separating out the constant. Numerically, we can simply set g to a small

number, which we have confirmed can accurately reproduce results for a neutral boson star.

In writing the final form of the static equations, we move to the metric variables σ and m defined in Eq. (7). The equations of motion are then

$$\begin{aligned} \phi'' &= -\left\{ \frac{2}{r} + \frac{4\pi Gr}{N} [(T_{\text{tot}})^r_r + (T_{\text{tot}})^t_t] + \frac{2Gm}{Nr^2} \right\} \phi' \\ &\quad - \frac{1}{N} \left(\frac{g^2 A_t^2}{N\sigma^2} - \mu^2 - 2\lambda\phi^2 \right) \phi \\ A_t'' &= \left\{ \frac{4\pi Gr}{N} [(T_{\text{tot}})^r_r - (T_{\text{tot}})^t_t] - \frac{2}{r} \right\} A_t' + \frac{2g^2}{N} A_t\phi^2, \end{aligned} \quad (25)$$

where $N = 1 - 2Gm/r$, and the energy-tensor components are

$$\begin{aligned} (T_b)^t_t &= -N\phi'^2 - \frac{g^2 A_t^2 \phi^2}{N\sigma^2} - \mu^2 \phi^2 - \lambda\phi^4 - \frac{A_t'^2}{2\sigma^2} \\ (T_b)^r_r &= +N\phi'^2 + \frac{g^2 A_t^2 \phi^2}{N\sigma^2} - \mu^2 \phi^2 - \lambda\phi^4 - \frac{A_t'^2}{2\sigma^2}. \end{aligned} \quad (26)$$

Charged boson stars are given by the solutions to Eqs. (25) and (8) with $(T_{\text{tot}})^{\mu\nu} = (T_b)^{\mu\nu}$. To solve these equations, we need inner and outer boundary conditions. For inner boundary conditions we require that the energy-momentum tensor be finite at the origin and thus $\mathcal{Q}(r) = O(r^2)$. Additional inner boundary conditions are found by plugging Taylor expansions of the fields into the equations of motion. We find $\phi(r) = \phi(0) + O(r^2)$, $A_t(r) = A_t(0) + O(r^2)$, $\sigma(r) = \sigma(0) + O(r^2)$ and $m = O(r^3)$. It helps with finding solutions to define

$$\hat{A}_t(r) \equiv \frac{A_t(r)}{\sigma(0)}, \quad \hat{\sigma}(r) \equiv \frac{\sigma(r)}{\sigma(0)}. \quad (27)$$

After replacing A_t and σ with \hat{A}_t and $\hat{\sigma}$, $\sigma(0)$ cancels out. Further, the inner boundary conditions are $\hat{A}_t(r) = \hat{A}_t(0) + O(r^2)$ and $\hat{\sigma}(r) = 1 + O(r^2)$ and $\sigma(0)$ no longer has to be known. How we determine $\hat{A}_t(0)$ will be explained in the next paragraph. To obtain outer boundary conditions, we require the energy-momentum tensor to go to zero at large r . We thus have $\phi, \phi', A_t' \rightarrow 0$ as $r \rightarrow \infty$.

Static solutions are uniquely identified by the central value $\phi(0)$. We thus specify a value for $\phi(0)$ and a trial value for $\hat{A}_t(0)$. We write the equations of motion in (25) in first order form and then integrate Eqs. (25) and (8) outward from $r = 0$ using the previously listed inner boundary conditions. We then vary $\hat{A}_t(0)$ using the shooting method until the outer boundary conditions are satisfied, at which point we have found a static solution.

Before presenting results, there are three additional quantities that are needed. These are equations for the total charge and mass of the star and our definition for the star's radius. As mentioned, the current in Eq. (21) is conserved, $\nabla_\mu J^\mu = 0$, which describes charge conser-

vation. The total charge inside a radius r is given by

$$- \int_0^r d^3r \sqrt{-g} J^t. \quad (28)$$

Using the bottom equation in (20), this can be integrated exactly and equals $\mathcal{Q}(r)$. Thus, as promised, $\mathcal{Q}(r)$ gives the total charge inside a radius r . The total charge in the system is given by $Q = \mathcal{Q}(\infty)$. Note that once a static solution is found, $\mathcal{Q}(r)$ is determined algebraically from Eq. (19),

$$\mathcal{Q}(r) = 4\pi r^2 \frac{\hat{A}'_t(r)}{\hat{\sigma}(r)}, \quad (29)$$

where both \hat{A}'_t and $\hat{\sigma}$ follow from the static solution.

To find an equation for the total mass of the star, we require that the spacetime be asymptotically Reissner-Nordström, so that in the large r limit

$$\frac{1}{a^2} \rightarrow 1 - \frac{2GM}{r} + \frac{G(Q^2/4\pi)}{r^2}, \quad (30)$$

which defines M , which we take to be the mass of the star. Comparing this to the definition of $m(r)$ in Eq. (7), we define

$$\mathcal{M}(r) \equiv m(r) + \frac{Q^2(r)}{8\pi r}, \quad (31)$$

so that $M = \mathcal{M}(\infty)$.

In the study of neutral boson stars, it is customary to define the radius of the star as the radius that contains some large percentage of the mass of the star. The same can be done with charged boson stars. We take the radius of the star to be R_{95} , which is the radius that contains 95% of the mass and is defined by

$$\mathcal{M}(R_{95}) = (0.95)M. \quad (32)$$

In presenting results, we use the quantities

$$\bar{M} \equiv \left(\frac{\mu}{10^{-10} \text{ eV}} \right) M, \quad \bar{R}_{95} \equiv \left(\frac{\mu}{10^{-10} \text{ eV}} \right) R_{95}, \quad (33)$$

which will be given in solar masses and kilometers, and

$$|\bar{\phi}(0)| \equiv \frac{1}{m_P} |\phi(0)|, \quad \bar{g} \equiv \frac{m_P}{\sqrt{8\pi}\mu} g, \quad (34)$$

which are dimensionless, where $m_P = 1/\sqrt{G}$ is the Planck mass. The factor of $\sqrt{8\pi}$ is included in the definition of \bar{g} so that it agrees with the scaled charge used in the literature [27, 28]. A nonrelativistic analysis suggests solutions only exist for $\bar{g}^2 < 1/2$, since otherwise the Coulomb repulsion is greater than the gravitational attraction [27]. This is not necessarily true in the relativistic case [28]. Nevertheless, we consider only $\bar{g} < 1/\sqrt{2} = 0.7071$.

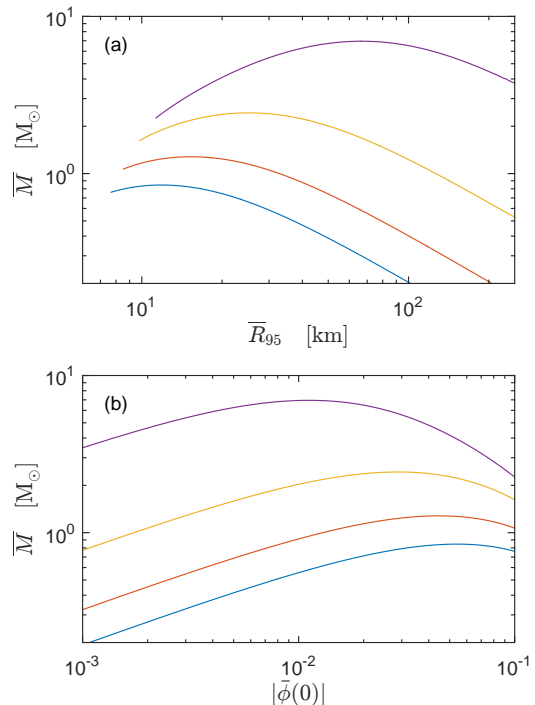


FIG. 2. (a) Mass-radius curves and (b) the mass as a function of the central value of the scalar field for charged boson stars. In both plots, the curves, from bottom to top, are for $\bar{g} = 0$ (blue), 0.5 (red), 0.65 (orange), and 0.7 (purple).

Some results are shown in Fig. 2. In Fig. 2(a) we show mass-radius curves for various values of \bar{g} . In Fig. 2(b) we show the mass as a function of the central (gauge-independent) value $|\bar{\phi}(0)|$. Many additional plots can be found in [28]. The transition from stable to unstable occurs at the critical solution. Since charged boson stars are single-fluid systems, the critical solution is the solution with the largest mass, just as with fermion stars. Solutions with central values of $|\bar{\phi}(0)|$ smaller than the critical value are stable, otherwise they are unstable. The critical values of $(|\bar{\phi}(0)|, M, R_{95})$ are (0.0541, 0.846 M_\odot , 11.9 km) for $\bar{g} = 0$, (0.0447, 1.28 M_\odot , 15.3 km) for $\bar{g} = 0.5$, (0.0288, 2.43 M_\odot , 25.1 km) for $\bar{g} = 0.65$, and (0.0112, 6.95 M_\odot , 66.7 km) for $\bar{g} = 0.7$. We can see that the critical solution can have its mass and radius increased significantly by increasing \bar{g} [27].

V. FERMION-CHARGED-BOSON STARS

In this section, we combine the equations from the previous sections and study fermion-charged-boson stars. As mentioned in the Introduction, we assume that non-gravitational interactions between the fermion and boson sectors are negligible. Consequently, the energy-momentum tensor separates [1],

$$(T_{\text{tot}})^\mu{}_\nu = (T_f)^\mu{}_\nu + (T_b)^\mu{}_\nu, \quad (35)$$

where $(T_f)^\mu{}_\nu$ and $(T_b)^\mu{}_\nu$ are as given in Eqs. (10) and (26) and are independently conserved,

$$\nabla_\mu(T_f)^\mu{}_\nu = 0, \quad \nabla_\mu(T_b)^\mu{}_\nu = 0, \quad (36)$$

which leads to the equations of motion given in Eqs. (11) and (25). We have also the metric equations in (8) and (9). The inner and outer boundary conditions are unchanged from those given in Secs. III and IV.

Static solutions are uniquely specified by the central pressure $p(0)$ for the fermion sector and the central value $\phi(0)$ for the boson sector. To solve the full system of equations, we specify values for $p(0)$ and $\phi(0)$ and a trial value for $\hat{A}_t(0)$. We then integrate outward from $r = 0$ and vary $\hat{A}_t(0)$ using the shooting method until the outer boundary conditions for the boson sector are satisfied, at which point we have found a static solution. During the integration, either p hits zero or ϕ drops to such a low value that it is effectively zero. When this happens, we break the integration and then restart it using only the single-fluid equations from either Sec. III or Sec. IV. The radius of the fermion part of the star, R_f , is defined as the radial position where the pressure hits zero, $p(R_f) = 0$. We consider this the visible radius, since it is the ordinary fermionic matter, and not dark matter, that is visible. The mass of the total system, M , is found using Eq. (31), but now $m(r)$ has contributions from both the fermion and boson sectors.

A. Stability

The first property we study is the stability of the static solutions with respect to small perturbations. In single-fluid systems, this is straightforward, since the transition from stable to unstable occurs at the static solution with the largest mass. As explained in Secs. III and IV, this solution is called the critical solution and it is identified by the critical central pressure, $p(0)$, for fermion stars and the critical central value for the scalar field, $|\phi(0)|$, for charged boson stars. The situation is not as straightforward for fermion–charged-boson stars, since static solutions are identified by both $p(0)$ and $|\phi(0)|$. As such, stability is no longer marked by a critical point, but instead a critical curve. One possibility for computing the critical curve is to write each field as a perturbation about its static value and then to solve the linearized system of equations. This has been done for fermion stars [34], boson stars [35–40], and charged boson stars [41], but not, as far as we are aware, for fermion-boson stars.

A simpler method for computing critical curves was presented in [14]. Critical curves satisfy

$$\frac{dM}{d\mathbf{p}} = \frac{dN_f}{d\mathbf{p}} = \frac{dN_b}{d\mathbf{p}} = 0, \quad (37)$$

where M is the mass of the system, N_f and N_b are the conserved fermionic and bosonic particle numbers, and \mathbf{p}

is a vector in parameter space. For details on the derivation of this result, we refer the reader to [14, 15, 42]. It can be shown that if two of the quantities in Eq. (37) are zero, then the third is also [14, 43]. One thing we note is that if we were to compute the critical curve by perturbing the system, we would only consider perturbations that conserve M , N_f , and N_b [34–37]. This is the reason why these quantities show up in Eq. (37).

Before explaining how we solve Eq. (37), we review how N_f and N_b are computed. It is worth stressing that N_f is the number of fluid elements and not, say, the number of baryons. The number density of fluid elements for the fermion sector, n_f , can be computed directly from the equation of state using [42]

$$n_f \propto \exp\left(\int \frac{d\epsilon}{\epsilon + p}\right), \quad (38)$$

where the proportionality constant does not affect the determination of stability and therefore does not have to be known. The total number of fermionic fluid elements inside a radius r , $\mathcal{N}_f(r)$, obeys

$$\mathcal{N}'_f = \frac{4\pi r^2 n_f}{\sqrt{N}}, \quad (39)$$

where $N = 1 - 2Gm/r$, and $N_f = \mathcal{N}_f(\infty)$. The equation above can be solved simultaneously with the equations of motion and metric equations. For the boson sector, N_b is the conserved particle number and is proportional to the conserved charge. Defining $\mathcal{N}_b(r) \equiv Q(r)/g$, the large r limit of \mathcal{N}_b gives N_b , or

$$N_b = \frac{Q}{g}. \quad (40)$$

To solve Eq. (37) we follow the methods presented in [15, 42]. We compute contour lines of either N_f or N_b in the full system. Moving along a single contour line, we determine the point where M is an extremum (in practice, we find that it is a maximum). These points give the critical curve.

Critical curves for $\mu = 10^{-10}$ eV and various values of \bar{g} are shown in Fig. 3(a). Each point in Fig. 3(a) represents a static solution. Those points that are inside the curve (i.e. the lower left region enclosed by the curve) represent stable solutions. For sufficiently small $|\phi(0)|$, we expect the star to be dominated by the fermion sector. Similarly, for sufficiently small $p(0)$, we expect the star to be dominated by the boson sector. In Fig. 3(a), we can see that for sufficiently small $|\phi(0)|$ or $p(0)$, the critical curves are trending towards, if not reproducing, the critical values reviewed in Secs. III and IV, as expected. The most interesting region of parameter space is when both $p(0)$ and $|\phi(0)|$ are relatively large, which occurs at the upper-right corner of the curves. Here we find that stability can be increased beyond the single-fluid critical values from Secs. III and IV. Indeed, we find that for larger \bar{g} , stability can be increased well beyond the single-fluid critical values of $|\phi(0)|$. The critical curves shown

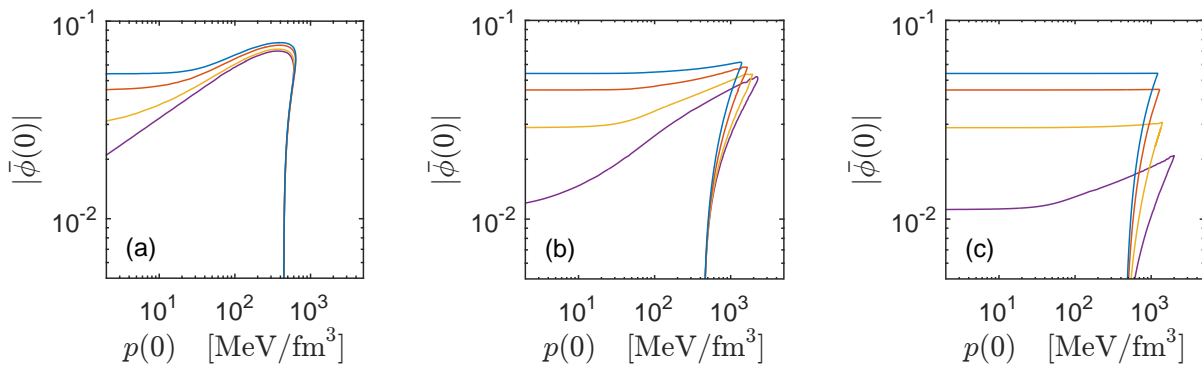


FIG. 3. Critical curves for (a) $\mu = 10^{-10}$ eV, (b) 10^{-9} eV, and (c) 10^{-8} eV. A point in each plot represents a static solution describing a fermion–charged-boson star. Those points inside the critical curve (i.e. the lower left region enclosed by the curve) represent stable solutions. In each plot, the curves, from top to bottom, are for $\bar{g} = 0$ (blue), 0.5 (red), 0.65 (orange), and 0.7 (purple).

in Fig. 3(a) are similar in shape to the critical curves for dark matter admixed neutron stars with fermionic dark matter [42].

Figures 3(b) and 3(c) show, respectively, critical curves for $\mu = 10^{-9}$ eV and $\mu = 10^{-8}$ eV. As the scalar field particle mass is increased we can see the extent to which the critical curve extends beyond the single-fluid critical value for $|\bar{\phi}(0)|$ is decreased. This can only occur if the fermion sector has a smaller influence over stability. We see also that the critical curve extends further beyond the single-fluid critical value for $p(0)$, indicating that the boson sector is having a larger influence over stability. We thus find that an increase in the scalar field mass leads to an increase in the role played by the boson sector for stability.

B. Fermion and boson contributions

It is useful to determine the relative contributions from the fermion and boson sectors to the star. In the original work on fermion-boson stars [1], this was studied in terms of the relative particle numbers. We choose instead to look at the relative contributions to the total mass. Since the mass of the star is measurable, it is interesting to determine how much the fermion and boson sectors contribute to such a measurement.

The solution to the bottom equation in (8) is m , which is used to find the mass of the star. This equation conveniently splits into $m = m_f + m_b$, where

$$m'_f \equiv -4\pi r^2 (T_f^t)_t, \quad m'_b \equiv -4\pi r^2 (T_b^t)_t. \quad (41)$$

From Eq. (31), we then have $\mathcal{M} = \mathcal{M}_f + \mathcal{M}_b$, where

$$\mathcal{M}_f \equiv m_f, \quad \mathcal{M}_b \equiv m_b + \frac{Q^2}{8\pi r}. \quad (42)$$

The total mass of the star can then be written as $M = M_f + M_b$, with the fermion and boson sector contribu-

tions given by

$$M_f \equiv \mathcal{M}_f(\infty), \quad M_b \equiv \mathcal{M}_b(\infty). \quad (43)$$

In Fig. 4, we show density plots for M_f/M , which is the contribution from the fermion sector to the total mass of the star. The upper row is for $\bar{g} = 0$ and for (a) $\mu = 10^{-10}$ eV, (b) 10^{-9} eV, and (c) 10^{-8} eV. The bottom row plots the same, but for $\bar{g} = 0.7$. Consider first the left column, where Figs. 4(a) and 4(d) have $\mu = 10^{-10}$ eV. We see a relatively wide transition from fermion domination (yellow) to boson domination (blue). In other words, the star is well mixed with fermions and bosons. This is exactly what we expected for $\mu = 10^{-10}$ eV from the simple analysis done in the Introduction. On the other hand, we see in the right column, where Figs. 4(c) and 4(f) have $\mu = 10^{-8}$ eV, that the transition is quite sharp. That the transition between fermion and boson domination sharpens as the scalar field mass is increased was first found in [1] for fermion–neutral-boson stars. Here we show that it continues to hold with charged scalar fields.

Superimposed on the plots in Fig. 4 are the critical curves from Fig. 3. Looking again at the right column, the yellow region is solidly dominated by the fermion sector, at least from the perspective of the total mass of the star. However, if the star were truly a single-fluid fermion star, then the vertical portion on the right side of critical curve would be straight. That the vertical portion on the right side bends outward indicates that the boson sector still has influence over the star, even though it has a negligible contribution to the total mass of the star.

C. Mass-radius diagrams

The last property we study are mass-radius diagrams. Once a static solution is found, the mass of the total system, M , and the radius of the fermion sector, R_f , are found as described at the beginning of this section. We

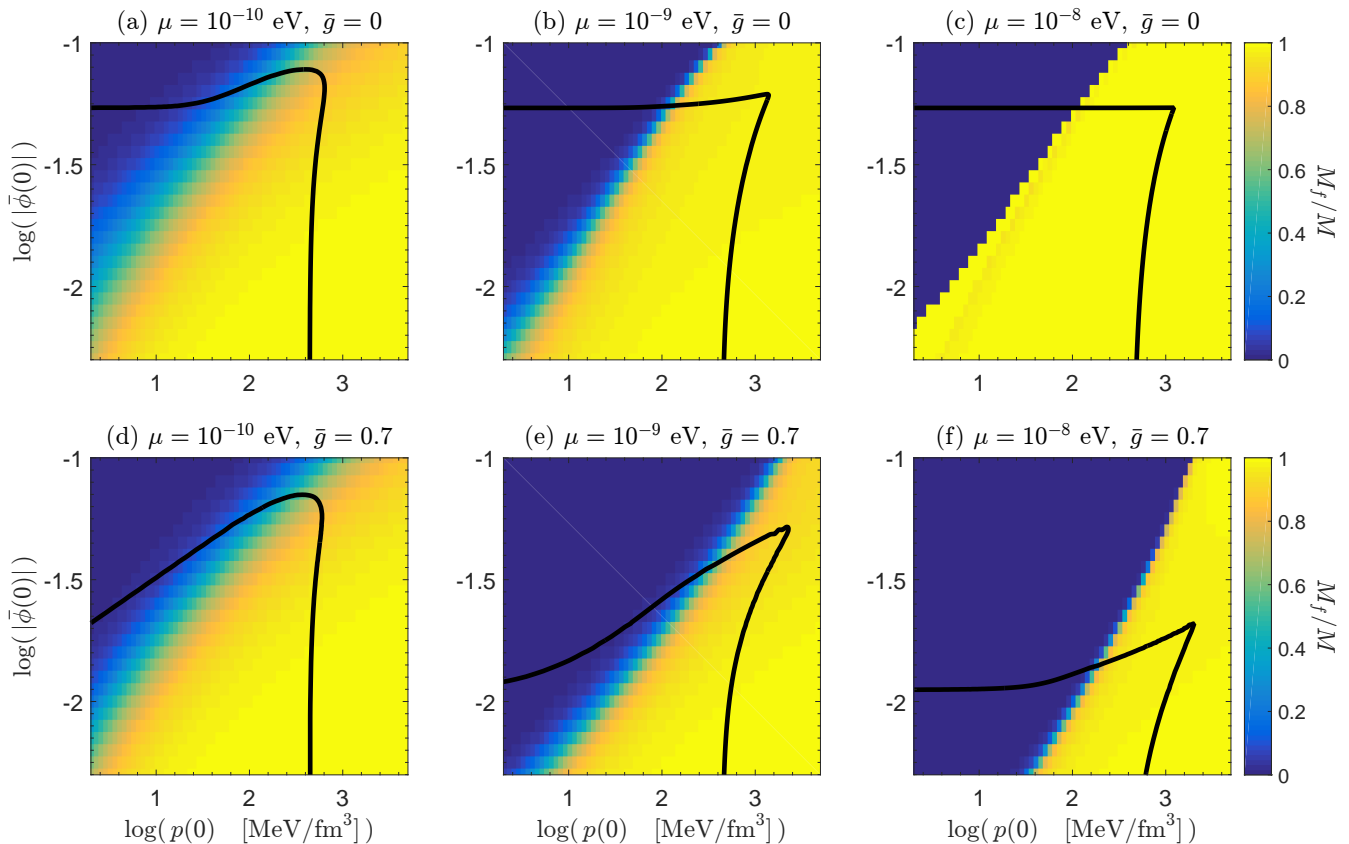


FIG. 4. The contribution from the fermion sector to the total mass of the star, M_f/M , is shown for various values of the scalar field mass, μ , and the scalar field charge, \bar{g} . These plots show the relative contribution to the total mass of the star from the boson and fermion sectors. Bright yellow indicates that the mass of the star is fermion dominated and dark blue indicates that it is boson dominated. The thick black curves are the critical curves from Fig. 3.

present results in terms of R_f , because R_f is the visible radius of the star since it is the ordinary fermionic matter that is the visible matter. Further, we present results only for $\mu = 10^{-10}$ eV.

In single-fluid systems, one has mass-radius curves, as shown in Figs. 1 and 2. With two-fluid fermion–charged-boson stars, the mass-radius relationship can no longer be represented by a single curve. In Fig. 5, we show mass-radius diagrams for the entirety of the stable parameter space shown in Fig. 3(a). In other words, for every stable point in Fig. 3(a), we compute the total mass and the radius of the fermion sector and plot this in Fig. 5. Figure 5 is analogous to the single-fluid plots in Figs. 1(a) and 2(a). For comparison, we have included the thick black curve, which is the mass-radius curve in Fig. 2(a), i.e. the mass-radius curve for a neutron star in the absence of dark matter.

We can see from Fig. 5 that the presence of the charged scalar field tends to decrease the visible radius of the star. As the charge of the scalar field is increased, this leads to larger possible masses. Thus, we find that fermion–charged-boson stars can be more compact and more mas-

sive than ordinary neutron stars.

In Fig. 6, we show mass diagrams, which are analogous to the single-fluid diagrams in Figs. 1(b) and 2(b). The thick black lines are the critical curves from Fig. 3(a). We can see that for sufficiently small $|\phi(0)|$ or $p(0)$, the total mass of the system is given by the single-fluid values, since in those regions the system is dominated by the fermion or boson sectors. This is consistent with what we have seen in the previous two subsections.

VI. CONCLUSION

We studied fermion–charged-boson stars, which are starlike systems with a mixture of fermions, as described by a perfect-fluid energy-momentum tensor and an equation of state, and bosons, as described by a charged complex scalar field. Fermion–charged-boson stars are examples of dark matter admixed neutron stars with bosonic dark matter.

In the fermion sector, we used the NL3 equation of state, which is a realistic equation of state for the ordi-

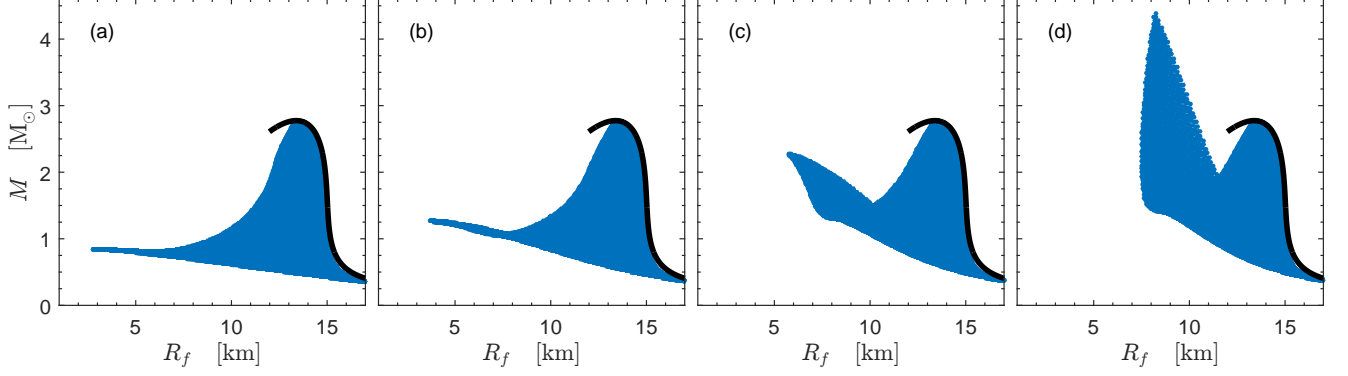


FIG. 5. Mass-radius diagrams for fermion–charged-boson stars with $\mu = 10^{-10}$ eV and (a) $\bar{g} = 0$, (b) 0.5, (c) 0.65, and (d) 0.7. M is the total mass of the star and R_f is the radius of the fermion sector, which is the visible radius of the star. The blue region gives the mass-radius relationships for the entirety of the stable parameter space shown in Fig. 3(a). For comparison, the thick black curve is included, which is the mass-radius curve in Fig. 2(a), i.e. the mass-radius curve for a neutron star in the absence of dark matter.

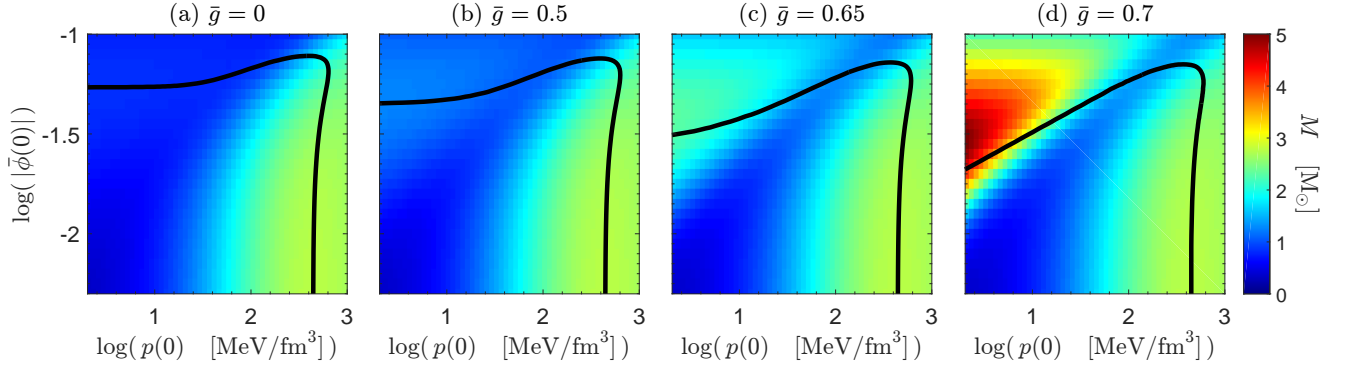


FIG. 6. Mass diagrams for fermion–charged-boson stars with $\mu = 10^{-10}$ eV and (a) $\bar{g} = 0$, (b) 0.5, (c) 0.65, and (d) 0.7. The thick black curves are the critical curves from Fig. 3(a)

nary nuclear matter in a neutron star, and in the boson sector, we focused on a scalar field mass of $\mu = 10^{-10}$ eV. We computed the critical curves, which show the stable region of parameter space. We then studied how the fermion and boson sectors contribute to the total mass of the star, finding that the transition sharpens as the scalar field mass is increased. Finally, we presented mass-radius and mass diagrams, finding that charged bosonic dark matter can lead to more massive and more compact stars as the charge is increased.

Appendix A: NL3 equation of state

In this appendix, we review the construction of the NL3 equation of state [32, 33]. The NL3 equation of state was used in the fermion sector throughout this paper and is constructed using relativistic mean field (RMF) theory. For matter content, we include protons, neutrons, electrons, and muons, as well as the scalar, vector, and vector-isovector mesons. We begin with a standard RMF

theory Lagrangian [2],

$$\mathcal{L}_{\text{ns}} = \mathcal{L}_B + \mathcal{L}_\sigma + \mathcal{L}_\omega + \mathcal{L}_\rho + \mathcal{L}_L, \quad (\text{A1})$$

where

$$\begin{aligned} \mathcal{L}_B &= \sum_{z=p,n} \bar{\psi}_z \left(i\gamma^\alpha \partial_\alpha - m_B + g_{B\sigma}\sigma \right. \\ &\quad \left. - g_{B\omega}\gamma^\alpha\omega_\alpha - \frac{1}{2}g_{B\rho}\gamma^\alpha\vec{\rho}_\alpha \cdot \vec{\tau} \right) \psi_z \\ \mathcal{L}_\sigma &= \frac{1}{2}\partial^\alpha\sigma\partial_\alpha\sigma - \frac{1}{2}m_\sigma^2\sigma^2 - \frac{\kappa}{3!}(g_{B\sigma}\sigma)^3 - \frac{\lambda}{4!}(g_{B\sigma}\sigma)^4 \\ \mathcal{L}_\omega &= -\frac{1}{4}\omega^{\alpha\beta}\omega_{\alpha\beta} + \frac{1}{2}m_\omega^2\omega^\alpha\omega_\alpha \\ \mathcal{L}_\rho &= -\frac{1}{4}\vec{\rho}^{\alpha\beta} \cdot \vec{\rho}_{\alpha\beta} + \frac{1}{2}m_\rho\vec{\rho}^\alpha \cdot \vec{\rho}_\alpha \\ \mathcal{L}_L &= \sum_{z=e,\mu} \bar{\psi}_z (i\gamma^\alpha\partial_\alpha - m_z) \psi_z, \end{aligned} \quad (\text{A2})$$

and

$$\begin{aligned}\omega_{\alpha\beta} &= \partial_\alpha\omega_\beta - \partial_\beta\omega_\alpha \\ \vec{\rho}_{\alpha\beta} &= \partial_\alpha\vec{\rho}_\beta - \partial_\beta\vec{\rho}_\alpha - g_\rho(\vec{\rho}_\alpha \times \vec{\rho}_\beta).\end{aligned}\quad (\text{A3})$$

ψ_z , with $z = p, n, e, \mu$, are the wave functions for the proton, neutron, electron, and muon, B labels the common baryon mass and couplings, σ is the scalar meson, v_α is the vector meson, and $\vec{\rho}_\alpha$ is the vector-isovector meson. We use the NL3 parameter set to fix the constants [32, 33]:

$$\begin{aligned}m_B &= 938 \text{ MeV} \\ m_\sigma &= 508.194 \text{ MeV} \\ m_\omega &= 782.5 \text{ MeV} \\ m_\rho &= 763 \text{ MeV} \\ g_{B\sigma}^2 &= 104.3871 \\ g_{B\omega}^2 &= 165.5854 \\ g_{B\rho}^2 &= 79.6 \\ \kappa &= 3.8599 \text{ MeV} \\ \lambda &= -0.01591.\end{aligned}\quad (\text{A4})$$

In RMF models, all non-fermionic fields are replaced with their mean field values: $\sigma \rightarrow \langle\sigma\rangle$, $\omega_\alpha \rightarrow \langle\omega_\alpha\rangle$, and $\vec{\rho}_\alpha \rightarrow \langle\vec{\rho}_\alpha\rangle$ [2]. This effectively reduces the system to a theory of free fermions which is straightforward to quantize. We do not review the quantization here, but simply state the results. The only nonvanishing mean fields are $\langle\sigma\rangle$, $\langle\omega_0\rangle$, and $\langle\rho_{03}\rangle$. The energy density and pressure are

$$\begin{aligned}\epsilon &= +\frac{1}{2}m_\sigma^2\langle\sigma\rangle^2 + \frac{\kappa}{3!}(g_{B\sigma}\langle\sigma\rangle)^3 + \frac{\lambda}{4!}(g_{B\sigma}\langle\sigma\rangle)^4 \\ &+ \frac{1}{2}m_\omega^2\langle\omega_0\rangle^2 + \frac{1}{2}m_\rho^2\langle\rho_{03}\rangle^2 \\ &+ \frac{1}{8\pi^2}\sum_z m_{*z}^4 \left[x_z \sqrt{1+x_z^2} (2x_z^2+1) \right. \\ &\quad \left. - \ln\left(x_z + \sqrt{1+x_z^2}\right) \right]\end{aligned}\quad (\text{A5})$$

and

$$\begin{aligned}p &= -\frac{1}{2}m_\sigma^2\langle\sigma\rangle^2 - \frac{\kappa}{3!}(g_{B\sigma}\langle\sigma\rangle)^3 - \frac{\lambda}{4!}(g_{B\sigma}\langle\sigma\rangle)^4 \\ &+ \frac{1}{2}m_\omega^2\langle\omega_0\rangle^2 + \frac{1}{2}m_\rho^2\langle\rho_{03}\rangle^2 \\ &+ \frac{1}{24\pi^2}\sum_z m_{*z}^4 \left[x_z \sqrt{1+x_z^2} (2x_z^2-3) \right. \\ &\quad \left. + 3 \ln\left(x_z + \sqrt{1+x_z^2}\right) \right],\end{aligned}\quad (\text{A6})$$

where the sums are over all fields, the general expression for an effective mass is

$$m_{*z} = m_z - g_{z\sigma}\langle\sigma\rangle \quad (\text{A7})$$

(with $g_{z\sigma} \neq 0$ for $z = p, n$), and $x_z \equiv k_z/m_{*z}$, where k_z is the Fermi momentum for particle z . The number densities are given by $n_z = k_z^3/3\pi^2$ and the chemical potentials are

$$\begin{aligned}\mu_p &= g_{B\omega}\langle\omega_0\rangle + g_{B\rho}I_{3p}\langle\rho_{03}\rangle + \sqrt{k_p^2 + m_{*p}^2} \\ \mu_n &= g_{B\omega}\langle\omega_0\rangle + g_{B\rho}I_{3n}\langle\rho_{03}\rangle + \sqrt{k_n^2 + m_{*n}^2} \\ \mu_e &= \sqrt{k_e^2 + m_e^2} \\ \mu_\mu &= \sqrt{k_\mu^2 + m_{*\mu}^2},\end{aligned}\quad (\text{A8})$$

where $I_{3p} = 1/2$ for the proton and $I_{3n} = -1/2$ for the neutron. The mean field values are obtained through their equations of motion,

$$\begin{aligned}m_\omega^2\langle\omega_0\rangle &= g_{B\omega}\sum_{z=p,n} n_z \\ m_\rho^2\langle\rho_{03}\rangle &= g_{B\rho}\sum_{z=p,n} I_{3z}n_z\end{aligned}\quad (\text{A9})$$

and

$$\begin{aligned}m_\sigma^2\langle\sigma\rangle &+ \frac{\kappa}{2}g_{B\sigma}^3\langle\sigma\rangle^2 + \frac{\lambda}{6}g_{B\sigma}^4\langle\sigma\rangle^3 \\ &= g_{B\sigma}\sum_{z=p,n} \frac{m_{*z}^3}{2\pi^2} \left[x_z \sqrt{1+x_z^2} - \ln\left(x_z + \sqrt{1+x_z^2}\right) \right].\end{aligned}\quad (\text{A10})$$

The equation of state, $p(\epsilon)$, for the core is computed by solving the above equations, under the assumption of beta equilibrium, which constrains the chemical potentials to obey $\mu_n = \mu_p + \mu_e$ and $\mu_e = \mu_\mu$, and charge neutrality, which requires $n_p = n_e + n_\mu$, using standard techniques [2]. At the critical baryonic number density $n_B^c = 0.052 \text{ fm}^{-3}$ [33], the core meets the inner crust. We describe the inner crust using a polytropic equation of state [44],

$$p(\epsilon) = A + B\epsilon^{4/3}, \quad (\text{A11})$$

where A and B are constants. A and B are determined by matching Eq. (A11) with the core at the critical baryonic number density and with the outer crust at the neutron drip line. For the outer crust we use the Baym-Petchick-Sutherland (BPS) equation of state [45, 46].

[1] A. B. Henriques, A. R. Liddle, and R. G. Moorhouse, COMBINED BOSON - FERMION STARS, Phys. Lett. B **233**, 99 (1989).

[2] N. K. Glendenning, *Compact Stars: Nuclear Physics, Particle Physics, and General Relativity*, 2nd ed. (Springer, New York, 2000).

- [3] D. J. Kaup, Klein-Gordon Geon, *Phys. Rev.* **172**, 1331 (1968).
- [4] R. Ruffini and S. Bonazzola, Systems of selfgravitating particles in general relativity and the concept of an equation of state, *Phys. Rev.* **187**, 1767 (1969).
- [5] P. Jetzer, Boson stars, *Phys. Rept.* **220**, 163 (1992).
- [6] F. E. Schunck and E. W. Mielke, General relativistic boson stars, *Class. Quant. Grav.* **20**, R301 (2003), arXiv:0801.0307 [astro-ph].
- [7] S. L. Liebling and C. Palenzuela, Dynamical Boson Stars, *Living Rev. Rel.* **15**, 6 (2012), arXiv:1202.5809 [gr-qc].
- [8] D. Akerib *et al.* (LUX), Limits on spin-dependent WIMP-nucleon cross section obtained from the complete LUX exposure, *Phys. Rev. Lett.* **118**, 251302 (2017), arXiv:1705.03380 [astro-ph.CO].
- [9] X. Cui *et al.* (PandaX-II), Dark Matter Results From 54-Ton-Day Exposure of PandaX-II Experiment, *Phys. Rev. Lett.* **119**, 181302 (2017), arXiv:1708.06917 [astro-ph.CO].
- [10] E. Aprile *et al.* (XENON), Dark Matter Search Results from a One Ton-Year Exposure of XENON1T, *Phys. Rev. Lett.* **121**, 111302 (2018), arXiv:1805.12562 [astro-ph.CO].
- [11] F. Sandin and P. Ciarcelluti, Effects of mirror dark matter on neutron stars, *Astropart. Phys.* **32**, 278 (2009), arXiv:0809.2942 [astro-ph].
- [12] S. Leung, M. Chu, and L. Lin, Dark-matter admixed neutron stars, *Phys. Rev. D* **84**, 107301 (2011), arXiv:1111.1787 [astro-ph.CO].
- [13] A. B. Henriques, A. R. Liddle, and R. G. Moorhouse, Combined Boson - Fermion Stars: Configurations and Stability, *Nucl. Phys. B* **337**, 737 (1990).
- [14] A. B. Henriques, A. R. Liddle, and R. G. Moorhouse, Stability of boson - fermion stars, *Phys. Lett. B* **251**, 511 (1990).
- [15] S. Valdez-Alvarado, C. Palenzuela, D. Alic, and L. A. Ureña-López, Dynamical evolution of fermion-boson stars, *Phys. Rev. D* **87**, 084040 (2013), arXiv:1210.2299 [gr-qc].
- [16] F. Di Giovanni, S. Fakhry, N. Sanchis-Gual, J. C. Degollado, and J. A. Font, Dynamical formation and stability of fermion-boson stars, *Phys. Rev. D* **102**, 084063 (2020), arXiv:2006.08583 [gr-qc].
- [17] S. Valdez-Alvarado, R. Becerril, and L. A. Ureña López, Fermion-boson stars with a quartic self-interaction in the boson sector, *Phys. Rev. D* **102**, 064038 (2020), arXiv:2001.11009 [gr-qc].
- [18] F. Di Giovanni, S. Fakhry, N. Sanchis-Gual, J. C. Degollado, and J. A. Font, A stabilization mechanism for excited fermion-boson stars, (2021), arXiv:2105.00530 [gr-qc].
- [19] C. M. G. de Sousa and J. L. Tomazelli, A Model for stars of interacting bosons and fermions, *Phys. Rev. D* **58**, 123003 (1998), arXiv:gr-qc/9507043.
- [20] F. Pisano and J. L. Tomazelli, Stars of WIMPs, *Mod. Phys. Lett. A* **11**, 647 (1996), arXiv:gr-qc/9509022.
- [21] K. Sakamoto and K. Shiraiishi, Exact solutions for boson fermion stars in (2+1)-dimensions, *Phys. Rev. D* **58**, 124017 (1998), arXiv:gr-qc/9806040.
- [22] C. M. G. de Sousa and V. Silveira, Slowly rotating boson fermion stars, *Int. J. Mod. Phys. D* **10**, 881 (2001), arXiv:gr-qc/0012020.
- [23] A. B. Henriques and L. E. Mendes, Boson - fermion stars: Exploring different configurations, *Astrophys. Space Sci.* **300**, 367 (2005), arXiv:astro-ph/0301015.
- [24] V. Dzhunushaliev, V. Folomeev, and D. Singleton, Chameleon stars, *Phys. Rev. D* **84**, 084025 (2011), arXiv:1106.1267 [astro-ph.SR].
- [25] R. Brito, V. Cardoso, and H. Okawa, Accretion of dark matter by stars, *Phys. Rev. Lett.* **115**, 111301 (2015), arXiv:1508.04773 [gr-qc].
- [26] R. Brito, V. Cardoso, C. F. B. Macedo, H. Okawa, and C. Palenzuela, Interaction between bosonic dark matter and stars, *Phys. Rev. D* **93**, 044045 (2016), arXiv:1512.00466 [astro-ph.SR].
- [27] P. Jetzer and J. J. van der Bij, CHARGED BOSON STARS, *Phys. Lett. B* **227**, 341 (1989).
- [28] D. Pugliese, H. Quevedo, J. A. Rueda H., and R. Ruffini, On charged boson stars, *Phys. Rev. D* **88**, 024053 (2013), arXiv:1305.4241 [astro-ph.HE].
- [29] S.-J. Sin, Late time cosmological phase transition and galactic halo as Bose liquid, *Phys. Rev. D* **50**, 3650 (1994), arXiv:hep-ph/9205208.
- [30] P.-H. Chavanis and T. Harko, Bose-Einstein Condensate general relativistic stars, *Phys. Rev. D* **86**, 064011 (2012), arXiv:1108.3986 [astro-ph.SR].
- [31] W. Hu, R. Barkana, and A. Gruzinov, Cold and fuzzy dark matter, *Phys. Rev. Lett.* **85**, 1158 (2000), arXiv:astro-ph/0003365.
- [32] G. A. Lalazissis, J. Konig, and P. Ring, A New parametrization for the Lagrangian density of relativistic mean field theory, *Phys. Rev. C* **55**, 540 (1997), arXiv:nucl-th/9607039.
- [33] B. G. Todd-Rutel and J. Piekarewicz, Neutron-Rich Nuclei and Neutron Stars: A New Accurately Calibrated Interaction for the Study of Neutron-Rich Matter, *Phys. Rev. Lett.* **95**, 122501 (2005), arXiv:nucl-th/0504034.
- [34] S. Chandrasekhar, The Dynamical Instability of Gaseous Masses Approaching the Schwarzschild Limit in General Relativity, *Astrophys. J.* **140**, 417 (1964), [Erratum: *Astrophys. J.* **140**, 1342 (1964)].
- [35] M. Gleiser, Stability of Boson Stars, *Phys. Rev. D* **38**, 2376 (1988), [Erratum: *Phys. Rev. D* **39**, 1257 (1989)].
- [36] P. Jetzer, Dynamical Instability of Bosonic Stellar Configurations, *Nucl. Phys. B* **316**, 411 (1989).
- [37] M. Gleiser and R. Watkins, Gravitational Stability of Scalar Matter, *Nucl. Phys. B* **319**, 733 (1989).
- [38] T. D. Lee and Y. Pang, Stability of Mini - Boson Stars, *Nucl. Phys. B* **315**, 477 (1989), [129(1988)].
- [39] S. H. Hawley and M. W. Choptuik, Boson stars driven to the brink of black hole formation, *Phys. Rev. D* **62**, 104024 (2000), arXiv:gr-qc/0007039.
- [40] B. Kain, Boson stars and their radial oscillations, *Phys. Rev. D* **103**, 123003 (2021), arXiv:2106.01740 [gr-qc].
- [41] P. Jetzer, Stability of Charged Boson Stars, *Phys. Lett. B* **231**, 433 (1989).
- [42] B. Kain, Dark matter admixed neutron stars, *Phys. Rev. D* **103**, 043009 (2021), arXiv:2102.08257 [gr-qc].
- [43] P. Jetzer, Stability of Combined Boson - Fermion Stars, *Phys. Lett. B* **243**, 36 (1990).
- [44] J. Carriere, C. J. Horowitz, and J. Piekarewicz, Low mass neutron stars and the equation of state of dense matter, *Astrophys. J.* **593**, 463 (2003), arXiv:nucl-th/0211015.
- [45] G. Baym, C. Pethick, and P. Sutherland, The Ground state of matter at high densities: Equation of state and stellar models, *Astrophys. J.* **170**, 299 (1971).
- [46] S. B. Ruester, M. Hempel, and J. Schaffner-Bielich, The outer crust of non-accreting cold neutron stars, *Phys.*

